Two-band second moment model and an interatomic potential for caesium

Graeme J. Ackland and Stewart K. Reed
School of Physics, The University of Edinburgh, James Clerk Maxwell Building, The King's Buildings, Mayfield Road, Edinburgh EH9 3JZ, United Kingdom

(Received 9 December 2002; published 19 May 2003)

A semiempirical formalism is presented for deriving interatomic potentials for materials such as caesium or cerium which exhibit volume collapse phase transitions. It is based on the Finnis-Sinclair second-moment tight-binding approach, but incorporates two independent bands on each atom. The potential is cast in a form suitable for large-scale molecular dynamics, the computational cost being the evaluation of short-ranged pair potentials. Parameters for a model potential for caesium are derived and tested.

DOI: 10.1103/PhysRevB.67.174108 PACS number(s): 61.72.−y, 64.60.−i, 34.20.Cf

I. INTRODUCTION

Semiempirical models for metallic binding have had a long and successful history in computer modeling. The most significant development came in the mid 1980s with the implementation of ''embedded atom'' method[1] (EAM) based loosely on density-functional theory[2] and ''*N*-body'' potentials[3] based on the tight-binding second-moment approximation.[4]

Although the rationale for these potentials suggests applicability to free-electron and transition-metal systems, respectively, the implied functional form is similar in each case. A large number of successful parametrizations of the functional forms suggested by these methods have been used, and they have established themselves as the standard method for modeling metallic systems.

In the second-moment approximation to tight binding, the cohesive energy is proportional to the square root of the bandwidth, which can be approximated as a sum of pairwise potentials representing squared hopping integrals. Assuming atomic charge neutrality, this argument can be extended to all band occupancies and shapes.[5] For simplicity, consider a rectangular *d* band of full width *W* centered on the atomic energy level E_0. The energy for this band relative to the free atom (the *bond energy*) is given by

$$U_{bond}=\int_{-W/2}^{E_f=(n/N-1/2)W} E\frac{N}{W}dE=\frac{W}{2N}n(n-N), \qquad (1)$$

where *n* is the occupation of the band and *N* is the capacity (for *d* bands $N=10$, for *s* bands $N=2$). The bandwidth is proportional to the square root of the second moment of the density of states. If we project the density of states onto each atom, and assume that each atom is charge neutral then the energy becomes

$$U_{bond}=\sum_i \int_{-W_i/2}^{E_f=(n/N-1/2)W_i} E\frac{N}{W_i}dE=-\sum_i \frac{W_i}{2N}n(N-n) \qquad (2)$$

and the second moment of the density of states can be calculated as the sum of the squares of the hopping integrals to nearest neighbors. This latter operation can be written as a sum of pair potentials,

$$W_i=\sqrt{\sum_j \phi(r_{ij})}. \qquad (3)$$

The enormous success of Finnis-Sinclair (and embedded atom-type) potentials arises from their extreme computational efficiency: essentially they are no more computationally expensive than a conventional pair potential. This allows them to be applied to extremely large-scale simulations, addressing complex geometries and phenomena which are intractable with more accurate quantum-mechanical models.

The computational simplicity follows from the formal division of the energy into a sum of energies per *atom*, which can in turn be evaluated locally. Here we follow a similar philosophy to Finnis-Sinclair, seeking to incorporate as much of the relevant physics as possible, without increasing the computational cost.

The alkali and alkaline-earth metals appear at first glance to be close-packed metals, forming fcc, hcp, or bcc structures at ambient pressures. However, compared with transition metals they are easily compressible, and at high pressures adopt more complex ''open'' structures (with smaller interatomic distances). The simple picture of the physics here is of a transfer of electrons from an *s* to a *d* band,[6–9] the *d* band being more compact but higher in energy. Hence, at the price of increasing their *energy U*, atoms can reduce their *volume V*, and since the stable structure at 0 K is determined by minimum *enthalpy* $H=U+PV$ at high pressure this transfer becomes energetically favorable. The net result is a metal-metal phase transformation characterized by a large reduction in volume (and often also in conductivity), the crystal structure itself is not the primary order parameter, and in some cases the transition may even be isostructural.

The mechanism of the phase transition is unknown. Although it is obvious that an isostructural phase transition is accompanied by an instability of the bulk modulus, the onset of this instability may occur after that in the shear modulus. Thus the mechanism may involve shearing rather than isostructural collapse, particularly if a continuous interface between the two phases exists, as in a shockwave.[10]

II. THE TWO-BAND MODEL

A. Energies

The Finnis-Sinclair formalism has been successfully used to study a large variety of systems. However, we are inter-

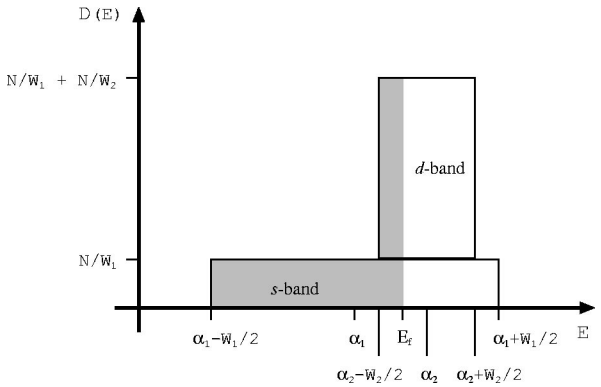

FIG. 1. The schematic picture of density of states (DOS) in a rectangular two-band model. Shaded region shows those energy states actually occupied.

ested in systems in which electrons change from one type of orbit to another and in particular, from an *s*-type orbital to a *d*-type orbital as the sample is pressurized.

Consider therefore two rectangular bands of widths W_1 and W_2 as shown in Fig. 1 with widths evaluated using Eq. (3). The bond energy of an atom may be written as the sum of the bond energies of the two bands on that atom as in Eq. (2), and a third term giving the energy of promotion from band 1 to band 2 [see Eq. (6)]:

$$U_{bond}=\sum_i \frac{W_{i1}}{2N_1}n_{i1}(n_{i1}-N_1)+\frac{W_{i2}}{2N_2}n_{i2}(n_{i2}-N_2)+E_{prom}, \tag{4}$$

where N_1 and N_2 are the capacities of the bands and n_{i1} and n_{i2} are the numbers of electrons in each band on the ith atom.

For an element, enforcing charge neutrality, the sum of the numbers of electrons is necessarily constrained to be equal to the total number of electrons on an atom,

$$n_{i1}+n_{i2}=T. \tag{5}$$

The difference between the energies of the band centers α_1 and α_2 is assumed to be fixed. The values of α correspond to the appropriate energy levels in the isolated atom. Thus, $\alpha_2-\alpha_1$ is the excitation energy from one level to another. For alkali and alkaline-earth metals, the free atom occupies only *s* orbitals, so the promotion energy term is therefore simply

$$E_{prom}=n_2(\alpha_2-\alpha_1)=n_2E_0, \tag{6}$$

where $E_0=\alpha_2-\alpha_1$.

Thus the band energy can be written as a function of n_{i1}, n_{i2} and the bandwidths (evaluated at each atom as a sum of pair potentials, within the second-moment approximation). Defining

$$\eta_i=n_{i1}-n_{i2} \tag{7}$$

and using Eq. (5) we can write:

$$U_{bond}=\sum_i -\frac{\eta_i}{4}(W_{i1}-W_{i2})-\frac{T}{4}(W_{i1}+W_{i2}) + \frac{\eta_i^2+T^2}{8}\left(\frac{W_{i1}}{N_1}+\frac{W_{i2}}{N_2}\right) + \frac{\eta_i T}{4}\left(\frac{W_{i1}}{N_1}-\frac{W_{i2}}{N_2}\right)+\frac{T-\eta_i}{2}E_0, \tag{8}$$

Although this expression looks unwieldy, it is in fact computationally efficient, requiring for its evaluation only two sums of pair potentials for W [see Eq. (3)] and a minimization *at each site independently* with respect to η_i. Since they are local variables, it is possible to write closed-form analytic expressions for η_i which minimize the total energy exactly, and so the energy is perfectly conserved [see Eq. (14)].

In addition to the bonding term, the Finnis-Sinclair form includes a pairwise repulsion between the ions, which is primarily due to the screened ionic charge and orthogonalization of the valence electrons. In the present case, this pair potential should be a function of η_i. In keeping with maintaining locality of the energy we write the pairwise contribution to the energy in the intuitive form, as the sum of two terms, one from each ''band,'' proportional to the number of electrons in that band:

$$V(r_{ij})=(n_{i1}+n_{j1})V_1(r_{ij})+(n_{i2}+n_{j2})V_2(r_{ij}). \tag{9}$$

We rearrange this to give the energy as a sum over atoms,

$$U_{pair}=\sum_i \left[n_{i1}\sum_{j\neq i}V_1(r_{ij})+n_{i2}\sum_{j\neq i}V_2(r_{ij})\right]. \tag{10}$$

The total energy is now simply

$$U_{tot}=U_{pair}+U_{bond}. \tag{11}$$

This depends on η_i, but as described above the η_i take the values that minimize the energy and one can solve:

$$\frac{\partial U_{tot}}{\partial \eta_i}=0 \tag{12}$$

explicitly for η_{i_0} *independently* at each atom, hence

$$\eta_{i_0}=\frac{N_1N_2}{W_{i1}N_2+W_{i2}N_1}\left[W_{i1}-W_{i2}-T\left(\frac{W_{i1}}{N_1}-\frac{W_{i2}}{N_2}\right)+2E_0 - 2U_{i1,pair}+2U_{i2,pair}\right]. \tag{13}$$

Depending on the number of electrons in the system it may not be possible to realize this. Charge neutrality requires that $|\eta_i|$ cannot be greater than the total number of electrons T per atom. The fixed capacities of the bands (N_1 and N_2) can also prohibit the realization of η_{i_0}. It is therefore necessary to limit the values which η_i may have:

$$\eta_i = \begin{cases} \min(T, 2N_1 - T) & \text{if } \eta_{i_0} > \min(T, 2N_1 - T) \\ \max(-T, T - 2N_2) & \text{if } \eta_{i_0} < \max(-T, T - 2N_2) \\ \eta_{i_0} & \text{otherwise} \end{cases} \tag{14}$$

where η_{i_0} is given by Eq. (13). The expressions for η_i involve only constants and sums of pair potentials, and can be evaluated independently at each atom at a similar computational cost to a standard many-body-type potential.

B. Forces

We use the variational property expressed in Eq. (12) to derive the force on the i^{th} atom:

$$\mathbf{f}_i = -\frac{dU_{tot}}{d\mathbf{r}_i} = -\left.\frac{\partial U_{tot}}{\partial \mathbf{r}_i}\right|_{\eta} - \frac{\partial U_{tot}}{\partial \eta}\frac{\partial \eta}{d\mathbf{r}_i} = -\left.\frac{\partial U_{tot}}{\partial \mathbf{r}_i}\right|_{\eta}. \tag{15}$$

Hence the force is simply the derivative of the energy at fixed η. Basically, this is the Hellmann-Feynman theorem,[11] which arises here because η is essentially a single-parameter representation of the electronic structure.

This result means that, like the energy, the force can be evaluated by summing pairwise potentials. Hence, the model is well suited for large-scale molecular dynamics.

The force derivation is somewhat tedious (see Appendix B), the result being

$$\mathbf{f}_i = \sum_j \left[(\tilde{W}_{i1} + \tilde{W}_{j1})\phi_1'(r_{ij}) + (\tilde{W}_{i2} + \tilde{W}_{j2})\phi_2'(r_{ij}) - (n_{i1} + n_{j1})\mathbf{V}_1'(r_{ij}) - (n_{i2} + n_{j2})\mathbf{V}_2'(r_{ij})\right]\hat{\mathbf{r}}_{ij} \tag{16}$$

with

$$\tilde{W}_{ib} = \frac{n_{ib}(N_b - n_{ib})}{4N_b W_{ib}}$$

and where the numbers of electrons in each band, n_{ib}, have been calculated analytically using Eqs. (13), (14), and (7). The contribution to the force from each neighbor acts along the direction of the vector between the atoms.

III. A MODEL POTENTIAL FOR CAESIUM

One application of the model is to simulate the pressure-induced isostructural phase transition in materials such as caesium. Here the transformation arises from electronic transition from the *s* to the *d* band. Caesium adopts the bcc structure (Cs I) at ambient pressure, transforming under slight additional pressure to fcc (Cs II) and under further increase transforming isostructurally to fcc (Cs III).[12,13] Here we seek to represent the volume collapse Cs II→Cs III transition.

A. Parametrization

To make a usable potential, the functional forms of ϕ and V must be chosen. Although this is somewhat arbitrary, the physical picture of the hopping integral and screened ion-ion potential suggests that both should be short ranged, continuous, and reasonably smooth.

TABLE I. Parameters for the two-band model, obtained by fitting to phases II and III of caesium.

	s band		*d* band
C_s	0.056 17 eV^2 Å^{-3}	C_d	0.1681 eV^2 Å^{-3}
d_s	9.5097 Å	d_d	6.9189 Å
A_s	2.4017×10^7 eV Å^{12}	A_d	3.7668×10^6 eV Å^{12}
	E_0		1.19 eV

In the present case, we are interested in the gross features of the model, so we adopt simple forms fitted to the cohesive energies and volume of the high- and low-pressure polytypes of caesium. For more complex applications, it may be necessary to fit other properties.

Following Finnis and Sinclair, we choose for the hopping integral

$$\phi_b(r_{ij}) = \begin{cases} C_b(d_b - r_{ij})^3 & \text{if } r_{ij} \leqslant d_b \\ 0 & \text{if } r_{ij} > d_b \end{cases} \tag{17}$$

and for the pairwise part, following Lennard-Jones,

$$V_b(r_{ij}) = \sum_j \frac{A_b}{r_{ij}^{12}}, \tag{18}$$

where *b* labels the band.

We select the promotion energy E_0 to be that required to promote an electron from the $6s$ level into the $5d$ level of an isolated atom.[14,15] The band capacities are $N_s = 2, N_d = 10$ and the total number of electrons per atom is $T = 1$. The cutoff radii d_s and d_d are chosen to be between the second and third nearest neighbors and between the first and second nearest neighbors, respectively. The remaining four parameters (A_s, A_d, C_s, C_d) are available for fitting.

Ab initio calculations using pseudopotentials, plane waves, and the generalized gradient approximation[16,17] show that the energy-volume relations for bcc and fcc caesium are almost degenerate, so we have fitted the remaining parameters to the atomic volumes of Cs I (115.9 Å^3/atom), Cs II (67.5 Å^3/atom), and Cs III (48.7 Å^3/atom) (Ref. 14) as well as the transition pressure between phases II and III (4.3 GPa) (Ref. 14) and the cohesive energy of phase I (-0.704 eV). The cohesive energy is the sum of the heat of formation and the heat of vaporization.[14]

Initial estimates for the parameters were determined using a symbolic mathematics package. The final parameters were arrived at by an iterative process: Least squares, conjugate gradients, and *ab oculo* minimization techniques were used to determine the best parameters for particular cutoff radii. The cutoff radii were then adjusted by hand to improve the fit. This process was repeated until the optimum fit was achieved. The final parameters are given in Table I.

Figure 2 shows the energy-volume curves for the fcc and bcc structures calculated using the model. The fcc structure is stable everywhere compared to the bcc structure. Experi-

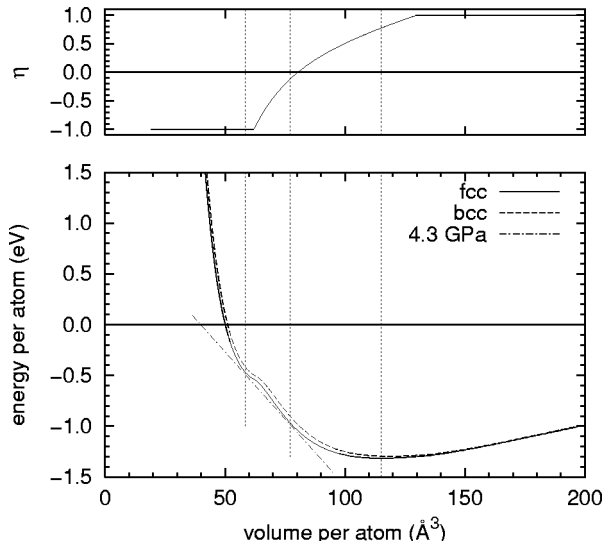

FIG. 2. Top: Variation of η_i with compression, showing $s \rightarrow d$ transfer in model caesium ($T=1$). Bottom: An energy-volume curve for the two-band potential. The minimum lies at -1.3163 eV and 115.2 Å^3/atom. The gradient of the straight dash-dotted line is the experimental fcc-fcc transition pressure. In reality, caesium also has a bcc-fcc phase transition at 2.3 GPa, however, the first-principles calculations show that these two structures are almost degenerate in energy at 0 K. The isostructural transition, which involves electron localization and hence is not properly reproduced by standard electronic structure calculation, occurs at 4.3 GPa.

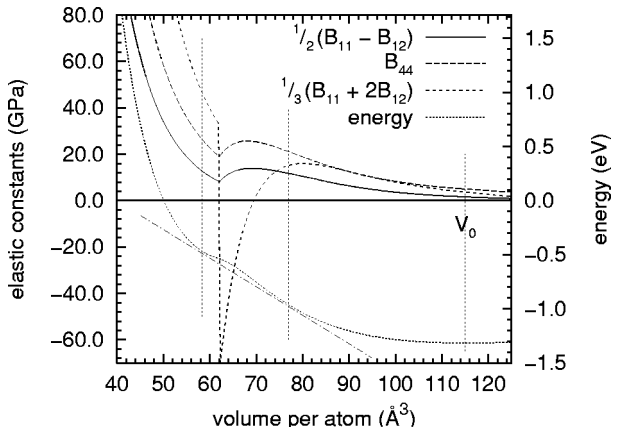

FIG. 3. The graph of elastic stiffness constants against volume. Mechanical instabilities occur for negative values of B_{44}, $(B_{11}-B_{12})/2$, and $(B_{11}+2B_{12})/3$. Total energy is shown on the same figure but with respect to the right-hand axis. The right most vertical line indicates the volume at ambient pressure. The other two vertical lines delineate the volumes in which the structure is unstable with respect to decomposition into coexisting phases, while the straight dash-dotted line is the transition pressure from phase II to phase III.

mentally, however, Cs I has bcc structure with an equilibrium volume of 116 Å^3. The present potential does not have a low-pressure bcc phase. However, at ambient pressure the bcc and fcc curves are almost degenerate (0.02 eV/atom difference) in agreement with the *ab initio* calculations. The predicted equilibrium volume of the ambient pressure phase agrees well with the experimental equilibrium volume of phase I of caesium. Although the predicted volumes of phases II and III are larger than the experimental values, the predicted transition pressure and volume collapse are in good agreement with experiment.

B. Elasticity

The elastic moduli are not fitted explicitly, so their behavior represents a sensitive test of the model. Application of the pressure generalization of the Born stability criteria is rather confused in the present literature,[18–20] so we lay this out in Appendix A.

Since caesium exhibits an isostructural phase transition, the bulk modulus must formally become negative at some volume (where the structure is unstable). It is less clear whether the other Born stability criteria will be violated: *ab initio* density-functional perturbation-theory calculations[17] find an instability in the long-range acoustic phonons; at zero pressure this is equivalent to an instability in $C'=(C_{11}-C_{12})/2$.

With the present potential the analytic expressions for the elastic constants are complicated: there is no simplification akin to Eq. (15) for the second derivatives. Consequently, we evaluate the elastic constants numerically from finite strain calculations, see Fig. 3. We find that the volume collapse is announced by a slight softening of the bulk modulus which then goes negative in the unstable region. Although the shear and tetragonal shear moduli decrease in the unstable region, neither actually goes negative.

C. Defects

One of the major features of many-body and embedded atom-type potentials is their ability to describe defects such as surfaces, vacancies, and interstitials without the constraints of pair potentials, for which the undercoordination defect energy is simply the sum of broken bond energies, less a small amount from the relaxation of atomic positions. Thus the vacancy formation energy is typically the same as the cohesive energy, whereas in real materials it is typically less than half. The present potential is not fitted to any defect configuration, so it is of interest to see what it predicts—moreover, the variety of environments associated with defects provides a good check against pathologies.

The relaxed surface energies for four low-energy surfaces are given in Table II. As is usual with many-body potentials the energy is much lower than would be expected from

TABLE II. Surface energies and atomic relaxations of the top two layers in angstroms.

Surface	Energy (meV/Å^2)	Relaxation (1 Å)	Relaxation (2 Å)
111	5.938	−0.042	0.000
001	6.54	−0.046	−0.007
011	7.195	0.024	−0.015
211	6.952	−0.122	−0.045

TABLE III. Interstitial and vacancy formation energies. The vacancy formation volume is 0.846 V_0.

Configuration	Energy eV
111 dumbbell	2.178
001 dumbbell	1.776
011 dumbbell	1.975
011 crowdion	1.975
Vacancy	0.545

simple bond counting. For the (111) surface the energy for each atom in the plane is increased by about 1/9 of its cohesive energy, while each atom has 1/4 of its bonds broken. There is also transfer of all electrons from *d*-like to *s*-like states at the free surface. This also leads to an unusual outwards relaxation of the surface atoms. Likewise the vacancy formation energy and volume (Table III) are rather typical of many-body potential results.

The interstitial formation energy is especially low (Table III), around 1.8 eV depending on the orientation and the amount of relaxation allowed locally, meaning that thermal interstitial formation is possible. This low value is due to the transfer of electrons from *s* to *d* band on the interstitial atom or dumbbell, similar to the high-pressure behavior. Consistent with recent *ab initio* calculations in various elements,[21–23] the calculated interatomic spacing of the dumbbell atoms is much smaller than in the bulk (around 15%) and much smaller than is typical of standard EAM-type potentials. As a consequence of this, the associated strain fields are considerably smaller.

For a detailed study of point defects in caesium, it would be appropriate to reparametrize the potential with point defects included in the fitting, but the good results obtained here without such fitting suggest that the present model contains the right physics.

IV. EXTRAPOLATION TO TRANSITION METALS

In principle, the current formalism should be applicable to *d*-band metals. We do not intend to refit the potentials here, but by applying the parameters fitted for caesium with appropriate scaling for ionic charge, and simply varying the total number of electrons we recover the parabolic behavior of the cohesive energy and bulk modulus, which characterizes the transition-metal series. Considering that there are no fitting parameters, the agreement with experimental results is extraordinarily good (Fig. 4). Moreover, the volume collapse phase transition exists only for $N=1$ and $N=2$ (consistent with experiment). However, since no information about band shape is included, the sequence of crystal structures cannot be reproduced, so we consider here only the fcc structures, calculating their ''experimental'' values from the experimental density.

While the extrapolated potentials do not represent the optimal parametrization for specific transition metals, the recovery of the trends across the group lends weight to the idea that the two-band model correctly reproduces the physics of this series.

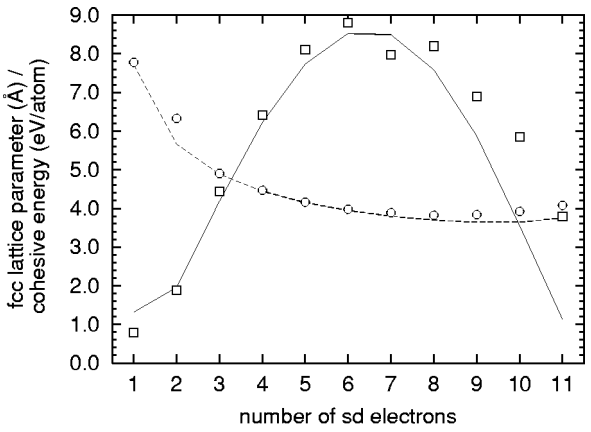

FIG. 4. The extrapolation of model to various $6s5d$-band materials. The parameters E_0, A_s, A_d, C_s, C_d, d_s, and d_d are taken from the fit to caesium, with the lengths being scaled according to the Fermi vector ($Z^{-1/3}$) and the energies by ($Z^{1/2}$). The lattice parameters are shown by the dashed line (calculated) and squares (experiment) and the cohesive energies by the solid line (calculated) and circles (experiment). Calculations are actually done at integer values of T and lines join these points. Agreement is somewhat poorer at high-Z where the amount of sd hybridization is not fully captured in the parametrization.

V. CONCLUSIONS

We have presented a model to describe $s \rightarrow d$ transfer within the framework of the empirical second-moment tight-binding model. With a very simple parametrization, our model describes the isostructural phase transition and associated $s \rightarrow d$ transfer in Cs and allows study of the elastic instabilities that occur under pressure and uniaxial stress. Throughout, our formalism is guided by the principle of retaining as much electronic detail as possible within the constraint of the computational complexity of short-ranged pair potentials.

Our potential form involves evaluation of sums of pair potentials, and minimization of the energy with respect to band occupation. In the approximation of local density of states evaluated at each atom, it becomes possible to formally write the energy of each atom in terms of the local band occupation, a single parameter η_i. This variational parameter can be explicitly eliminated from the energy and force expressions, meaning that energies and forces can be evaluated by summing pair potentials.

To our knowledge, the present potential represents the most sophisticated energy function which uses first derivatives which are analytic pair potentials, exploiting Hellman-Feynman theorem in empirical potentials to achieve this. It is thus uniquely well suited for exploitation in standard molecular-dynamics codes. It is interesting to contrast our work with similar approaches based on valence bond or extended Huckel theory: there the energy is associated with a two-site bond, and in principle there are N^2 of these, so one has to assume a constant bonding topology or deal with nonlocal bond breaking.[29,30]

Extension of the formalism to transition metals is straightforward, and the caesium parametrization gives a surpris-

ingly good description across the group. While providing impressive proof of concept, this may not be of enormous practical use, however, since once there is a significant partial occupation of the *d* band under all conditions the model is similar to the standard many-body potentials which are known to do a good job in describing transition metals.[24]

The precise stable crystal symmetry depends on the shape of the band structure, and is not therefore correctly described in this rectangular band model. Many-body potentials never contain the correct physics to describe phase transitions, except in the martensitic case of freezing in soft phonons.[25,26] However, the crystal structure which has the lowest energy can be determined by the judicious choice of functions V and ϕ. Here the simple use of the power-law repulsion and cubic attraction leads to close-packed structures. We find that the phase transition in caesium does not arise from a mechanical instability of the crystal: the mechanical stability criteria are satisfied until well beyond the point of thermodynamic instability. Thus there will be considerable hysteresis in the transition pressure at low temperature.

The two-band formalism can be easily combined with alternate parametrizations to get effective band shapes, and could be applied to ferromagnetic systems where the two bands represent separate spins, and the atomic E_0 term is replaced by a term that favors maximum spin.

APPENDIX A: ELASTIC INSTABILITIES UNDER PRESSURE-ENERGY DEFINITION

There is a degree of confusion in the literature regarding the definition of elastic constants under pressure. To some extent this arises because of various definitions of strain (Lagrangian, Eulerian, volume conserving). Here we lay out the definitions in terms of energy. One important point to note is that under pressure the moduli which correspond to long-wavelength phonons are volume conserving, while those corresponding to crystal stability are not. At finite pressure, this means that they are different.

At pressure, the important quantity for stability in energetic terms is the Gibbs free energy G,

$$G = U - TS + PV, \tag{A1}$$

where P is an externally applied hydrostatic pressure. $U - TS$ is the Helmholtz free energy F. The change in the Gibbs energy due to a distortion of the crystal is

$$\Delta G = \Delta F + \Delta PV + P\Delta V. \tag{A2}$$

If the hydrostatic pressure is applied by an external mechanism, then ΔP is zero. Therefore,

$$\Delta G = \Delta F + P\Delta V. \tag{A3}$$

Any arbitrary change in the unit cell be expressed in terms of the strain tensor $\overleftrightarrow{\varepsilon}$. Using the Voigt notation, the matrix representation of the strain tensor is written as

$$\overleftrightarrow{\varepsilon} = \begin{pmatrix} e_1 & e_6/2 & e_5/2 \\ e_6/2 & e_2 & e_4/2 \\ e_5/2 & e_4/2 & e_3 \end{pmatrix}. \tag{A4}$$

If we write the equilibrium cell as a matrix comprising the three lattice vectors $\overleftrightarrow{V}_0 = (\mathbf{r}_1, \mathbf{r}_2, \mathbf{r}_3)$, then any arbitrary strain gives a new unit cell:

$$\overleftrightarrow{V} = \overleftrightarrow{V}_0(1 + \overleftrightarrow{\varepsilon}). \tag{A5}$$

If the volume of the original cell is $V_0 = |\overleftrightarrow{V}_0|$, then the volume of the new cell is

$$\begin{aligned} V/V_O &= |\overleftrightarrow{V}|/|\overleftrightarrow{V}_0| \\ &= 1 + e_1 + e_2 + e_3 + e_1e_2 + e_2e_3 + e_3e_1 - e_4^2/4 - e_5^2/4 \\ &\quad - e_6^2/4 + e_1e_2e_3 - e_1e_4^2/4 - e_2e_5^2/4 - e_3e_6^2/4 \\ &\quad + e_4e_5e_6/4, \end{aligned} \tag{A6}$$

which can be expressed concisely in standard strain notation (i,j,k,l representing Cartesian directions) as

$$\frac{\Delta V}{V} = e_{ii} + \frac{1}{4}(2\delta_{ij}\delta_{kl} - \delta_{ik}\delta_{jl} - \delta_{il}\delta_{jk})e_{ij}e_{kl} + O(\varepsilon^3) \tag{A7}$$

where δ_{ij} is the Kronecker delta and the usual implicit sum convention for tensors applies. The change in the Gibbs free energy may then be written as

$$\Delta G = \Delta F + Pe_{ii} + \frac{PV}{4}(2\delta_{ij}\delta_{kl} - \delta_{ik}\delta_{jl} - \delta_{il}\delta_{jk})e_{ij}e_{kl}. \tag{A8}$$

We define C_{ij} as the second-order derivatives of the Helmholtz free energy with respect to the Voigt strains and B_{ij} as the second-order derivatives of the Gibbs free energy with respect to the Voigt strains. The limiting case of long-wavelength phonons is related to C_{ij}, which can be calculated from the dynamical matrix,[27] the crystal stability criteria are related to the B_{ij}.[19] In the standard notation,

$$B_{ijkl} = C_{ijkl} + \frac{P}{2}(2\delta_{ij}\delta_{kl} - \delta_{ik}\delta_{jl} - \delta_{il}\delta_{jk}). \tag{A9}$$

In the Voigt notation,

$$B_{ij} = \begin{cases} C_{ii} - P/2 & \text{if } i = j \text{ and } i > 3 \\ C_{ij} + P & \text{if } i \neq j \text{ and } i,j < 4. \\ C_{ij} & \text{otherwise} \end{cases} \tag{A10}$$

The Born elastic stability criteria restrict what values various moduli may have if the crystal is to be stable.[28] In the case of external pressure the relevant free energy is G and the relevant moduli are B_{ij}. Due to the Voigt symmetry, the elastic constant tensor has, in general, only 21 independent components. In cubic crystals, however, this number is further reduced by symmetry to 3, namely B_{11}, B_{12}, and B_{44}.

Consequently, there are three common stability criteria which impose lower bounds on the bulk, shear, and tetragonal shear moduli of cubic crystals. These may be written in the Voigt notation as

$$\tfrac{1}{3}(B_{11}+2B_{12})>0, \quad B_{44}>0, \quad \text{and} \quad \tfrac{1}{2}(B_{11}-B_{12})>0. \tag{A11}$$

Whence the generalized Born stability criteria for the elastic constants of cubic crystals at pressure become

$$\tfrac{1}{3}(C_{11}+2C_{12}+2P)>0,$$

$$C_{44}-\frac{p}{2}>0, \ \frac{1}{2}(C_{11}-C_{12}-P)>0, \tag{A12}$$

where

$$B_{11}=C_{11}, \quad B_{12}=C_{12}+P, \quad \text{and} \quad B_{44}=C_{44}-\frac{p}{2}. \tag{A13}$$

Calculation of bulk, shear, and tetragonal shear moduli from energies

In this paper, we evaluate the elastic moduli by applying finite strain and measuring the change in total energy U_{tot}. The finite strain method has the advantage over analytic differentiation of automatically compensating for nonisotropic movement of the atoms. At zero temperature U_{tot} is the same as the classical Helmholtz free energy F. At finite pressure, however, the system is not at a minimum of U_{tot} with respect to strain.

When applying strain to a system under pressure, the first-order term in the Gibbs free energy vanishes:

$$\Delta G=e_{ij}\frac{\partial G}{\partial e_{ij}}+\frac{1}{2}e_{ij}e_{kl}\frac{\partial^2 G}{\partial e_{ij}\partial e_{kl}}=\frac{1}{2}e_{ij}e_{kl}\frac{\partial^2 G}{\partial e_{ij}\partial e_{kl}}. \tag{A14}$$

But the first-order term for Helmholtz does not. For a cubic crystal, one can find $(C_{11}+2C_{12})/3$, $(C_{11}-C_{12})/2$, and C_{44} directly at any volume by simple distortions and measurement of F.

For bulk modulus we apply a pair of the Voigt strains, with $e_1=e_2=e_3=e$, the other elements being zero. Assuming that we make a pair of small distortions about a volume V, the difference

$$G(e)+G(-e)-2G(0)=V\frac{(B_{11}+2B_{12})}{3}9e^2+O(e^3). \tag{A15}$$

Equivalently, using the Helmholtz free energy,

$$\frac{(C_{11}+2C_{12})}{3}=\frac{[F(e)+F(-e)-2F(0)]}{9Ve^2}+O(e^3). \tag{A16}$$

For $(C_{11}-C_{12})/2$, the relevant distortion, volume conserving to first order, is $e=e_1=-e_2$ and

$$\frac{(C_{11}-C_{12})}{2}=\frac{[F(e)+F(-e)-2F(0)]}{4Ve^2}+O(e^3). \tag{A17}$$

For C_{44}, the relevant distortion is $e=e_6$ and

$$C_{44}=\frac{[F(e)+F(-e)-2F(0)]}{Ve^2}+O(e^3). \tag{A18}$$

APPENDIX B: DERIVATION OF THE FORCE ON AN ATOM

Since the cohesive energy is variational with respect to the electron distribution η, the derivative of the energy with respect to the electron distribution is zero and so the force may be written as a partial derivative akin to the Hellmann-Feynman theorem.[11] From Eq. (15)

$$\mathbf{f}_i=\left.\frac{\partial U_{tot}}{\partial \mathbf{r}_i}\right|_{\eta}=-\sum_j \left.\frac{\partial U_j}{\partial \mathbf{r}_i}\right|_{\eta_j}. \tag{B1}$$

where the sum over j includes $j=i$. From Eqs. (4), (6), and (8), the cohesive energy of the jth atom in terms of the number of electrons in each band (n_{j1} and n_{j2}) is

$$U_j=\left[\frac{n_{j1}}{2}\left(\frac{n_{j1}}{N_1}-1\right)W_{j1}+\frac{n_{j2}}{2}\left(\frac{n_{j2}}{N_2}-1\right)W_{j2} + n_{j1}\sum_{k\neq j}V_1(r_{jk})+n_{j2}\sum_{k\neq j}V_2(r_{jk})+n_{j2}E_0\right], \tag{B2}$$

and the force on atom i is thus

$$\mathbf{f}_i=-\sum_j\left[\frac{n_{j1}}{2}\left(\frac{n_{j1}}{N_1}-1\right)\frac{\partial W_{j1}}{\partial \mathbf{r}_i}+\frac{n_{j2}}{2}\left(\frac{n_{j2}}{N_2}-1\right)\frac{\partial W_{j2}}{\partial \mathbf{r}_i} + \left(n_{j1}+n_{i1}\frac{\partial}{\partial \mathbf{r}_i}V_1(r_{ij})\right)+\left(n_{j2}+n_{i2}\frac{\partial}{\partial \mathbf{r}_i}V_2(r_{ij})\right)\right]. \tag{B3}$$

The width of band b on atom i is $W_{jb}=\sqrt{\Sigma_{k\neq j}\phi_b(r_{jk})}$ and its derivative is

$$\frac{\partial W_{jb}}{\partial \mathbf{r}_i}=\frac{1}{2W_{jb}}\sum_{k\neq j}\frac{\partial}{\partial \mathbf{r}_i}\phi_b(r_{jk}) =\begin{cases}\dfrac{1}{2W_{jb}}\displaystyle\sum_{k\neq j}\frac{\partial}{\partial \mathbf{r}_i}\phi_b(r_{jk}) & \text{if } j=i\\ \dfrac{1}{2W_{jb}}\dfrac{\partial}{\partial \mathbf{r}_i}\phi_b(r_{jk}) & \text{if } j\neq i.\end{cases} \tag{B4}$$

The pairwise terms are given in Eq. (9), the derivatives are straightforward, noting that an atom does not interact with itself so $V(r_{ii})=0$.

On combining the above equations, the force may then be written as

$$\mathbf{f}_i = -\sum_{j\neq i}\left[\frac{n_{j1}}{4W_{j1}}\left(\frac{n_{j1}}{N_1}-1\right)\frac{\partial\phi_1(r_{ji})}{\partial\mathbf{r}_i}+\frac{n_{j2}}{4W_{j2}}\left(\frac{n_{j2}}{N_2}-1\right)\frac{\partial\phi_2(r_{ji})}{\partial\mathbf{r}_i}+n_{j1}\frac{\partial V_1(r_{ji})}{\partial\mathbf{r}_i}+n_{j2}\frac{\partial V_2(r_{ji})}{\partial\mathbf{r}_i}\right]$$
$$-\left[\frac{n_{i1}}{4W_{i1}}\left(\frac{n_{i1}}{N_1}-1\right)\sum_{k\neq i}\frac{\partial\phi_1(r_{ik})}{\partial\mathbf{r}_i}+\frac{n_{j2}}{4W_{j2}}\left(\frac{n_{j2}}{N_2}-1\right)\sum_{k\neq i}\frac{\partial\phi_2(r_{ik})}{\partial\mathbf{r}_i}+n_{j1}\sum_{k\neq i}\frac{\partial V_1(r_{ik})}{\partial\mathbf{r}_i}+n_{j2}\sum_{k\neq i}\frac{\partial V_2(r_{ik})}{\partial\mathbf{r}_i}\right]. \quad \text{(B5)}$$

To simplify the appearance of this equation we define

$$\tilde{W}_{ib}=\frac{n_{ib}(N_b-n_{ib})}{4N_bW_{ib}} \quad \text{(B6)}$$

and the force becomes

$$\mathbf{f}_i=\sum_{j\neq i}\left[\tilde{W}_{j1}\frac{\partial\phi_1(r_{ji})}{\partial\mathbf{r}_i}+\tilde{W}_{j2}\frac{\partial\phi_2(r_{ji})}{\partial\mathbf{r}_i}-n_{j1}\frac{\partial V_1(r_{ji})}{\partial\mathbf{r}_i}-n_{j2}\frac{\partial V_2(r_{ji})}{\partial\mathbf{r}_i}\right]$$
$$+\sum_{k\neq i}\left[\tilde{W}_{i1}\frac{\partial\phi_1(r_{ik})}{\partial\mathbf{r}_i}+\tilde{W}_{i2}\frac{\partial\phi_2(r_{ik})}{\partial\mathbf{r}_i}-n_{j1}\frac{\partial V_1(r_{ik})}{\partial\mathbf{r}_i}-n_{j2}\frac{\partial V_2(r_{ik})}{\partial\mathbf{r}_i}\right]. \quad \text{(B7)}$$

The summations in the second set of square brackets may be reindexed in terms of j's and included in the first set of square brackets to give

$$\mathbf{f}_i=\sum_{j\neq i}\left[\tilde{W}_{j1}\frac{\partial\phi_1(r_{ji})}{\partial\mathbf{r}_i}+\tilde{W}_{j2}\frac{\partial\phi_2(r_{ji})}{\partial\mathbf{r}_i}-n_{j1}\frac{\partial V_1(r_{ji})}{\partial\mathbf{r}_i}-n_{j2}\frac{\partial V_2(r_{ji})}{\partial\mathbf{r}_i}\right.$$
$$\left.+\tilde{W}_{i1}\frac{\partial\phi_1(r_{ij})}{\partial\mathbf{r}_i}+\tilde{W}_{i2}\frac{\partial\phi_2(r_{ij})}{\partial\mathbf{r}_i}-n_{j1}\frac{\partial V_1(r_{ij})}{\partial\mathbf{r}_i}-n_{j2}\frac{\partial V_2(r_{ij})}{\partial\mathbf{r}_i}\right]. \quad \text{(B8)}$$

Since both ϕ and V are pair potentials, $\phi_b(r_{ij})=\phi_b(r_{ji})$ and $V_b(r_{ij})=V_b(r_{ji})$. The derivatives of ϕ are

$$\frac{\partial}{\partial\mathbf{r}_i}\phi_b(r_{ij})=\frac{\partial}{\partial r_i}\phi_b(r_{ij})\hat{\mathbf{r}}_{ij}=\phi_b'(r_{ij})\hat{\mathbf{r}}_{ij},$$

where the ϕ_b' are scalar quantities and $\phi_b'(r_{ij})=\phi_b'(r_{ji})$. Similarly, the derivatives of V are

$$\frac{\partial}{\partial\mathbf{r}_i}V_b(r_{ij})=\frac{\partial}{\partial r_i}V_b(r_{ij})\hat{\mathbf{r}}_{ij}=V_b'(r_{ij})\hat{\mathbf{r}}_{ij},$$

where again the V_b' are scalar quantities.

Finally, the force on atom i is then

$$\mathbf{f}_i=\sum_{j\neq i}\left[(\tilde{W}_{i1}+\tilde{W}_{j1})\phi_1'(r_{ij})+(\tilde{W}_{i2}+\tilde{W}_{j2})\phi_2'(r_{ij})\right.$$
$$\left.-(n_{i1}+n_{j1})V_1'(r_{ji})-(n_{i2}+n_{j2})V_2'(r_{ji})\right]\hat{\mathbf{r}}_{ij}. \quad \text{(B9)}$$

[1] M.S. Daw and M.I. Baskes, Phys. Rev. B **29**, 6443 (1984).
[2] P. Hohenberg and W. Kohn, Phys. Rev. **136**, B864 (1964).
[3] M.W. Finnis and J.E. Sinclair, Philos. Mag. A **50**, 45 (1984).
[4] F. Ducastelle, J. Phys. (Paris) **31**, 1055 (1970).
[5] G.J. Ackland, V. Vitek, and M.W. Finnis, J. Phys. F: Met. Phys. **18**, L153 (1988).
[6] K. Takemura, S. Minomura, and O. Shimomura, Phys. Rev. Lett. **49**, 1772 (1982).
[7] R. Boehler and M. Ross, Phys. Rev. B **29**, 3673 (1984).
[8] M.M. Abd-Elmeguid, H. Pattyn, and S. Bukshpan, Phys. Rev. Lett. **72**, 502 (1994).
[9] A.K. MacMahan, Phys. Rev. B **29**, 5982 (1984).
[10] K. Kadau, T.C. Germann, P.S. Lomdahl, and B.L. Holian, Science (Washington, DC, U.S.) **296**, 1681 (2002).
[11] R. Feynman, Phys. Rev. **56**, 340 (1939).
[12] H.T. Hall, L. Merrill, and J.D. Barnett, Science (Washington, DC, U.S.) **146**, 1297 (1964).
[13] There is some recent evidence that the Cs III phase may be a more complex structure, see M.I. McMahon, R.J. Nelmes, and S. Rekhi, Phys. Rev. Lett. **87**, 255502 (2001).
[14] *CRC Handbook of Chemistry and Physics*, 74th ed., edited by D.R. Lide (CRC Press, Boca Raton, FL, 1993).
[15] S.P. Bates (private communication).
[16] S.K. Reed, Ph.D. thesis, University of Edinburgh.
[17] J. Xie, S.P. Chen, J.S. Tse, D.D. Klug, Z. Li, K. Uehara, and L.G. Wang, Phys. Rev. B **62**, 3624 (2000).
[18] J. Wang, S. Yip, S.R. Phillpot, and D. Wolf, Phys. Rev. Lett. **71**, 4182 (1993).
[19] B.B. Karki, G.J. Ackland, and J. Crain, J. Phys.: Condens. Matter **9**, 8579 (1997).

[20] P.M. Marcus, H. Ma, and SL. Qui, J. Phys.: Condens. Matter **14**, L525 (2002).
[21] S.W. Han, L. Ruiz-Zapeta, G.J. Ackland, R. Car, and D. Srolovitz, Phys. Rev. B **66**, 220101 (2002).
[22] E. Smargiassi and P.A. Madden, Phys. Rev. B **51**, 129 (1995).
[23] C. Domain and C.S. Becquart, Phys. Rev. B **65**, 024103 (2002).
[24] G.J. Ackland, G.I. Tichy, V. Vitek, and M.W. Finnis, Philos. Mag. A **56**, 735 (1987).
[25] U. Pinsook and G.J. Ackland, Phys. Rev. B **58**, 11252 (1998).
[26] U. Pinsook and G.J. Ackland, Phys. Rev. B **62**, 5427 (2000).
[27] S.J. Clark and G.J. Ackland, Phys. Rev. B **48**, 10899 (1993).
[28] M. Born and K. Huang, *Dynamical Theory of Crystal Lattices* (Oxford University Press, Oxford, 1966).
[29] A. Chen and L.R. Corrales, J. Non-Cryst. Solids **249**, 81 (1999); J. Chem. Phys. **104**, 4632 (1996).
[30] G.J. Ackland, Phys. Rev. B, **40**, 10351 (1989).